Published in final edited form as:
Neuron. 2003 July 17; 39(2): 227–239.

Huntingtin and Huntingtin-Associated Protein 1 Influence Neuronal Calcium Signaling Mediated by Inositol-(1,4,5) Triphosphate Receptor Type 1

Tie-Shan Tang[1], **Huiping Tu**[1], **Edmond Y.W. Chan**[3], **Anton Maximov**[2], **Zhengnan Wang**[1], **Cheryl L. Wellington**[4], **Michael R. Hayden**[3], and **Ilya Bezprozvanny**[1,*]

[1]Department of Physiology

[2]Center for Basic Neuroscience, University of Texas Southwestern, Medical Center at Dallas, Dallas, Texas 75390

[3]Center for Molecular Medicine and Therapeutics, Department of Medical Genetics, Children's and Women's Hospital

[4]Department of Pathology and Laboratory Medicine, University of British Columbia, Vancouver, British Columbia, Canada

Summary

Huntington's disease (HD) is caused by polyglutamine expansion (exp) in huntingtin (Htt). The type 1 inositol (1,4,5)-triphosphate receptor ($InsP_3R1$) is an intracellular calcium (Ca^{2+}) release channel that plays an important role in neuronal function. In a yeast two-hybrid screen with the $InsP_3R1$ carboxy terminus, we isolated Htt-associated protein-1A (HAP1A). We show that an $InsP_3R1$-HAP1A-Htt ternary complex is formed in vitro and in vivo. In planar lipid bilayer reconstitution experiments, $InsP_3R1$ activation by $InsP_3$ is sensitized by Htt^{exp}, but not by normal Htt. Transfection of full-length Htt^{exp} or caspase-resistant Htt^{exp}, but not normal Htt, into medium spiny striatal neurons faciliates Ca^{2+} release in response to threshold concentrations of the selective mGluR1/5 agonist 3,5-DHPG. Our findings identify a novel molecular link between Htt and $InsP_3R1$-mediated neuronal Ca^{2+} signaling and provide an explanation for the derangement of cytosolic Ca^{2+} signaling in HD patients and mouse models.

Introduction

Huntington's disease (HD) has onset usually between 35 and 50 years with chorea and psychiatric disturbances and gradual but inexorable intellectual decline to death after 15–20 years (Vonsattel and DiFiglia, 1998). Neuropathological analysis reveals selective and progressive neuronal loss in the striatum (Vonsattel et al., 1985), particularly affecting the GABAergic medium spiny striatal neurons (MSNs). At the molecular level, the cause of HD is a polyglutamine (polyQ) expansion (exp) in the amino terminus of huntingtin (Htt), a 350 kDa ubiquitously expressed cytoplasmic protein (HDCRG, 1993; Nasir et al., 1996). A number of transgenic HD mouse models have been generated, which reproduce many HD-like features (Menalled and Chesselet, 2002; Rubinsztein, 2002). Despite significant progress, cellular mechanisms that link the mutation with the disease remain controversial (Tobin and Signer, 2000).

*Correspondence: ilya.bezprozvanny@utsouthwestern.edu.

A number of Htt binding partners have been identified in yeast two-hybrid (Y2H) screens with an Htt amino-terminal fragment (Gusella and MacDonald, 1998; Kalchman et al., 1997; Singaraja et al., 2002). Htt-associated protein-1 (HAP1) was the first identified Htt binding partner (Li et al., 1995; Gutekunst et al, 1998; Page at al, 1998). Importantly, the HD-causing polyQ expansion of Htt (Htt^{exp}) promotes Htt-HAP1 association (Li et al., 1995, 1998b). In rodents, two HAP1 protein isoforms differing in their carboxy termini are expressed via alternative splicing —HAP1A and HAP1B—both of which bind Htt (Li et al., 1995; Nasir et al., 1998). Only one HAP1 isoform has been identified in humans, and this is most similar to rodent HAP1A (Li et al., 1998b). Association of HAP1 with hepatocyte growth factor-regulated tyrosine kinase substrate (Hrs) (Li et al., 2002), the p150Glued subunit of dynactin (Engelender et al., 1997; Li et al., 1998a), and the Rac1 guanine nucleotide exchange factor Kalirin-7/Duo (Colomer et al., 1997) has been discovered in Y2H screens. Targeted disruption of the *HAP1* gene in mice results in postnatal death and depressed feeding behavior, suggesting an important role of HAP1 in hypothalamic function (Chan et al., 2002). Despite all these data, the role of HAP1 in neuronal signaling and the pathogenesis of HD remain unclear (Bertaux et al., 1998).

The inositol (1,4,5)-triphosphate receptor ($InsP_3R$) is an intracellular calcium (Ca^{2+}) release channel that plays an important role in neuronal Ca^{2+} signaling (Berridge, 1998). Three isoforms of $InsP_3R$ have been identified (Furuichi et al., 1994). The type 1 receptor ($InsP_3R1$) is the predominant neuronal isoform. Mice lacking $InsP_3R1$ display severe ataxic behavior (Matsumoto et al., 1996), and mice with a spontaneous mutation in the *$InsP_3R1$* gene experience convulsions and ataxia (Street et al., 1997), suggesting a major role of $InsP_3R1$ in neuronal function. To identify novel $InsP_3R1$ neuronal binding partners, we performed a Y2H screen of a rat brain cDNA library and isolated neuronal cytoskeleton 4.1N protein (Maximov et al., 2003) and HAP1A. In the present manuscript, we describe biochemical and functional interactions of $InsP_3R1$ with HAP1A and Htt. The discovered association of $InsP_3R1$ with HAP1A and Htt provides additional insight into HAP1 function in the brain and to our knowledge for the first time links neuronal $InsP_3R1$ function with Htt and HD.

Results

$InsP_3R1$ Binds to HAP1A in the Yeast Two-Hybrid System

We aimed to identify novel proteins that bind to the carboxy-terminal cytosolic region of the $InsP_3R1$. We used the carboxy-terminal region of rat $InsP_3R1$ in the pLexN vector (IC bait, amino acids D2590–A2749) for Y2H screening of a rat brain cDNA library and isolated 16 positive clones. The clones were rescued and tested for their strength of association with the IC bait in a liquid Y2H assay. Three of the 16 isolated clones displayed especially strong interaction with the IC bait. Two of the strongly interacting clones (clones 7 and 8) corresponded to neuronal cytoskeleton protein 4.1N (Maximov et al., 2003). The third strongly interacting clone (clone 11) corresponded to a partial fragment of HAP1A.

To systematically map the HAP1A-interacting domain, a number of $InsP_3R1$ carboxy-terminal fragments were cloned into pLexN vector, and the strength of interaction with clone 11 (partial HAP1A) was measured in a liquid Y2H assay (Figure 1A). From the obtained results we concluded that the minimal $InsP_3R1$ region required for interaction with HAP1A corresponds to amino acids F2627–G2736 (Figure 1A, shaded). Thus, the HAP1A-interacting domain in the $InsP_3R1$ carboxy-terminal region partially overlaps with the minimal 4.1N-interacting region (F2627–R2676; Figure 1A) and largely complements the minimal protein phosphatase 1α (PP1α) binding region (R2731–A2749; Figure 1A) mapped in our previous studies (Maximov et al., 2003; Tang et al., 2003).

Two carboxy-terminal splice variants of HAP1 protein are expressed in the rodent brain (Li et al., 1995). Clone 11 corresponds to a carboxy-terminal portion of the rat HAP1A isoform. To address whether both HAP1 isoforms bind $InsP_3R1$ with similar affinity, we cloned full-length rat HAP1A and HAP1B cDNAs into the Y2H vectors and tested their ability to associate with IC10 bait. We observed strong interaction between IC10 and either full-length HAP1A or clone 11 (Figure 1B). In contrast, the HAP1B isoform did not display any detectable inter-action with IC10. Thus, unique carboxy-terminal sequences present in HAP1A protein (K578–L599) appear to robustly modulate association with the IC10 bait.

$InsP_3R1$ Binds to HAP1A and Htt In Vitro

To confirm the $InsP_3R1$-HAP1 association, we performed a series of in vitro binding experiments. In the first experiments, we expressed GST-IC8 and GST-IC10 $InsP_3R1$ carboxy-terminal proteins in *E. coli* and performed GST pull-downs with extracts from COS7 cells transiently expressing hemagglutinin-tagged HAP1 proteins (HA-HAP1A and HA-HAP1B). In agreement with Y2H data, GST-IC10, but not GST-IC8, specifically associated with HA-HAP1A protein (Figure 1C). In further agreement with Y2H results, GST-IC10 association with HA-HAP1B was much weaker than that with HA-HAP1A (Figure 1C).

Do HAP1 proteins bind to full-length $InsP_3R1$? To address this, we expressed full-length $InsP_3R1$ (RT1) in Sf9 cells by baculovirus infection and performed in vitro binding experiments using lysates from COS7 cells transiently transfected with HA-HAP1A- or HA-HAP1B-expressing plasmids. The Sf9 and COS7 cell lysates were incubated together, precipitated with anti-$InsP_3R1$ polyclonal anti-bodies, and blotted with anti-HA monoclonal antibodies. In agreement with Y2H and GST pull-down experiments, full-length $InsP_3R1$ associated more strongly with HA-HAP1A than with HA-HAP1B (Figure 1D).

Since HAP1 interacts with Htt (Li et al., 1995), we investigated whether an $InsP_3R1$-HAP1A-Htt ternary complex might be formed. To explore this, we expressed full-length Htt-23Q or Htt-82Q proteins (Cooper et al., 1998) in HEK293 cells and performed GST pull-down experiments. We discovered that GST-IC10 protein, but not GST-IC8, efficiently precipitated Htt-82Q proteins from HEK293 cell lysates (Figure 1E). Compared to Htt-82Q, much smaller amounts of Htt-23Q were precipitated by GST-IC10 (Figure 1E). The addition of COS7 cell lysates containing overexpressed HA-HAP1A into the GST-IC10 pull-down reaction significantly increased the amount of precipitated Htt-23Q protein (Figure 1E), but had only a minor effect on the amount of precipitated Htt-82Q protein (Figure 1E). In control experiments we detected the expression of endogenous HAP1A protein in HEK293 cells (data not shown). One explanation of our findings is that Htt-82Q bound endogenous HAP1A with much higher affinity than Htt-23Q. As a result, endogenous levels of HAP1A in HEK293 cells were sufficient to support robust Htt-82Q, but not Htt-23Q, precipitation by GST-IC10. Alternatively, Htt-82Q, but not Htt-23Q, may be exhibiting strong and direct binding to the $InsP_3R1$ carboxy terminus, even in the absence of HAP1A (see Discussion).

$InsP_3R1$-HAP1-Htt Association In Vivo

We performed additional GST pull-down experiments with rat cerebellar and cortical lysates. In agreement with data using cultured cells, GST-IC10, but not GST-IC8, precipitated endogenous Htt from rat brain cerebellar and cortical lysates (Figure 2A). To address whether $InsP_3R1$ and Htt interacted in vivo, we performed coimmunoprecipitation experiments with rat brain cerebellar and cortical lysates using anti-$InsP_3R1$ polyclonal antibodies. In agreement with the pull-down data, endogenous Htt protein is coimmunoprecipitated with the $InsP_3R1$, even in the presence of GST-IC8 protein, which was added in the reaction (Figure 2B). In contrast to GST-IC8, inclusion of GST-IC10

protein into anti-$InsP_3R1$ immunoprecipitation reactions significantly reduced the amounts of precipitated Htt (Figure 2B). These results are consistent with the formation of an $InsP_3R1$-HAP1-Htt ternary complex in neurons within rat cerebellum and cortex regions. Similar results were obtained in experiments with rat striatal lysates (data not shown).

To determine the requirement of HAP1 for the $InsP_3R1$-Htt association, we studied brain extracts from mice with targeted disruption of HAP1 (Chan et al., 2002). In these experiments, brain extracts from $HAP1^{-/-}$ mouse pups and wild-type control littermates were used in immunoprecipitaion experiments with anti-$InsP_3R1$ polyclonal antibodies. The precipitated fractions were blotted with anti-Htt monoclonal antibodies. In agreement with the rat brain coimmunoprecipitation results, we found that anti-$InsP_3R1$ polyclonal antibodies specifically precipitated Htt from wild-type mouse cortical lysates (Figure 2C, left panel, third lane). Slightly reduced amounts of Htt protein were precipitated by anti-$InsP_3R1$ polyclonal antibodies from $HAP1^{-/-}$ cortical lysates (Figure 2C, right panel, third lane). To investigate preferentially strong protein-protein interactions, an additional 0.5 M KCl washing step was employed. The 0.5 M KCl wash did not appreciably decrease the amount of Htt precipitated by anti-$InsP_3R1$ antibodies from wild-type mouse brain extract (Figure 2C, left panel, fourth lane). In contrast, the high-salt wash drastically reduced the amount of Htt precipitated from $HAP1^{-/-}$ brain extracts (Figure 2C, right panel, fourth lane). From these results we concluded that the presence of HAP1 proteins is required for the formation of a high-affinity salt-resistant $InsP_3R1$-Htt association. Western blotting of anti-$InsP_3R1$ immunoprecipitates with HAP1 monoclonal antibodies confirmed the preferential binding of $InsP_3R1$ to the HAP1A isoform (Figure 2D, left panel) and the absence of both HAP1 isoforms in $HAP1^{-/-}$ samples (Figure 2D, right panel). The binding of $InsP_3R1$ to HAP1 was not significantly affected by the 0.5 M KCl wash (Figure 2D, left panel).

Htt^{exp}, but Not Normal Htt, Activates $InsP_3R1$ In Vitro

The HAP1 binding site and the site of polyQ expansion are localized to the most amino-terminal region of Htt protein (Li et al., 1995). We expressed amino-terminal fragments (Htt-N, amino acids 1–158) of Htt-15Q and Htt-138Q as GST-fusion proteins and confirmed association of Htt-N-15Q and Htt-N-138Q with HA-HAP1A (data not shown). We further demonstrated that bacterially expressed Htt-N-15Q and Htt-N-138Q proteins specifically precipitated recombinant full-length $InsP_3R1$ from Sf9 cell lysates (Figure 3A). Since Sf9 lysates do not contain any HAP1 (data not shown), this Htt-N interaction with full-length $InsP_3R1$ appears to be direct. Our GST-IC10 pull-down experiments (Figure 1E) and immunoprecipitation experiments from $HAP1^{-/-}$ cortical lysates (Figure 2C) also support the existence of a direct Htt-$InsP_3R1$ interaction. $InsP_3R1$ associated with Htt-N-138Q more strongly than with Htt-N-15Q (Figure 3A), although this difference was less dramatic than the difference between Htt-23Q and Htt-82Q in GST-IC10 pull-down experiments (Figure 1E).

What are the functional consequences of $InsP_3R1$ association with HAP1 and Htt? To address this, we expressed $InsP_3R1$ in Sf9 cells and reconstituted recombinant $InsP_3R1$ into planar lipid bilayers as previously described (Tang et al., 2003; Tu et al., 2002). Addition of 100 nM $InsP_3$ to the *cis* (cytosolic) chamber induced low levels of $InsP_3R1$ activity (Figure 3B, second trace, and Figure 3C). Further addition of GST protein or repetitive additions of Htt-N-15Q protein directly to the bilayer had no effect on $InsP_3R1$ activity (Figure 3B, traces 3–5, and Figure 3C). In contrast, addition of Htt-N-138Q protein to the same bilayer resulted in facilitation of $InsP_3R1$ activity (Figure 3B, trace 6, and Figure 3C). On average, $InsP_3R1$ open probability was equal to 0.020 ± 0.008 ($n = 16$) in the presence of 100 nM $InsP_3$, 0.02 ± 0.01 ($n = 6$) after addition of Htt-N-15Q, and 0.19 ± 0.05 ($n = 4$) after addition of Htt-N-138Q. The facilitation of $InsP_3R1$ activity by Htt-N-138Q was most pronounced at

low $InsP_3$ concentrations. When $InsP_3R1$ was activated by 2 μM $InsP_3$, additions of GST, Htt-N-15Q, and Htt-N-138Q proteins did not have a significant effect on $InsP_3R1$ open probability (Figure 3D). From these results, we concluded that Htt-N-138Q, but not Htt-N-15Q, sensitizes $InsP_3R1$ to activation by submaximal doses of $InsP_3$.

To evaluate the role of HAP1 in $InsP_3R1$ activation by Htt, we expressed and purified full-length HAP1A as a GST-fusion protein. Addition of HAP1A to the bilayer had no effect on the activity of $InsP_3R1$ in the presence of 100 nM $InsP_3$ (Figure 4A, third trace, and Figure 4B). In contrast to previous experiments (Figures 3B and 3C), addition of Htt-N-15Q to the bilayer pre-exposed to HAP1A facilitated $InsP_3R1$ activity (Figure 4A, fourth trace, and Figure 4B). The following addition of Htt-N-138Q to the same membrane had an additional potentiating effect (Figure 4A, trace 5, and Figure 4B). Similar results were obtained in the experiments when HAP1A was premixed with Htt-N-15Q or Htt-N-138Q prior to addition to the bilayer (data not shown). On average, $InsP_3R1$ open probability was equal to 0.020 ± 0.008 (n = 16) in the presence of 100 nM $InsP_3$, 0.14 ± 0.04 (n = 5) after addition of HAP1A + Htt-N-15Q, and 0.26 ± 0.11 (n = 5) after addition of HAP1A + Htt-N-138Q. From these in vitro functional experiments and our biochemical data, we concluded that HAP1A facilitates activation of $InsP_3R1$ by Htt, most likely by promoting Htt association with $InsP_3R1$ carboxy terminus (Figure 1E).

Since amino-terminal Htt fragments were used in bilayer experiments shown above, we determined the effect of full-length Htt on $InsP_3R1$ activity. We generated baculoviruses expressing full-length Htt-23Q and Htt-82Q and used them in coinfection experiments with RT1 baculovirus encoding $InsP_3R1$. In immunoprecipitation experiments we found that $InsP_3R1$ and Htt-23Q/82Q formed a complex when coexpressed in Sf9 cells (Figure 5A), which do not contain any detectable HAP1. As such, interaction of the $InsP_3R1$ with Htt23Q/82Q in Sf9 cells appears direct, consistent with our earlier findings. Similar to pull-down data gathered with the GST-Htt-N protein (Figure 3A), binding of Htt to full-length $InsP_3R1$ was only modestly modulated by polyQ expansion.

Microsomes prepared from Sf9 cells coinfected with RT1 and Htt-23Q or Htt-82Q baculoviruses were fused to planar lipid bilayers. No channel activity was observed in control experimental conditions (Figures 5B and 5D, first trace). Addition of 100 nM $InsP_3$ induced only low levels of channel activity in $InsP_3R1$ coexpressed with Htt-23Q (Figure 5B, second trace, and Figure 5C), but resulted in dramatic activation of $InsP_3R1$ coexpressed with Htt-82Q (Figure 5D, second trace, and Figure 5E). Elevation of $InsP_3$ concentration to 2 μM increased activity of $InsP_3R1$ coexpressed with Htt-23Q (Figure 5B, third trace, and Figure 5C) and had no additional effect on activity of $InsP_3R1$ coexpressed with Htt-82Q (Figure 5D, third trace, and Figure 5E). From these experiments we concluded that sensitivity of $InsP_3R1$ to activation by $InsP_3$ is increased by formation of a complex with Htt-82Q full-length protein, but not with Htt-23Q full-length protein.

Htt^{exp} Activates $InsP_3R1$ in Cultured MSNs

Striatal MSN neurons are the most selectively and severely affected in HD (Vonsattel et al., 1985). To test the in vivo functional effects of Htt^{exp} on $InsP_3R1$, we established primary MSN cultures from E18 embryonic rats (Mao and Wang, 2001). Over 90% of striatal neurons are projection GABAergic MSNs (Gerfen, 1992). A large fraction of cells in our cultures (>90%) were strongly positive for GAD65 marker in immunostaining experiments (data not shown), confirming their identity as MSNs (Chesselet et al., 1993; Mao and Wang, 2001). We transfected MSNs at 20 days in vitro (DIV) with full-length Htt-23Q, Htt-82Q, or Htt-138Q expression plasmids. To identify transfected cells, the Htt plasmids were cotransfected with enhanced green fluorescent protein (EGFP)-expressing plasmid. During transfections, the Htt:EGFP plasmid ratio was kept at 3:1 to ensure that every GFP-positive

cell was transfected with Htt-expressing plasmid. In control experiments, MSNs were transfected with the EGFP plasmid alone. Only GFP-positive cells were compared in our analysis of different Htt constructs.

In contrast to striatal interneurons, MSNs abundantly express phospholipase C (PLC)-linked mGluR1/5 receptors (Mao and Wang, 2001, 2002; Tallaksen-Greene et al., 1998). To stimulate $InsP_3R1$-mediated Ca^{2+} release, we challenged Fura-2-loaded MSN neurons with 10 μM 3,5-dihydroxyphenylglycine (DHPG), a specific mGluR1/5 receptor agonist (Mao and Wang, 2002; Schoepp et al., 1999). To exclude the contribution of *N*-methyl-D-aspartate receptors (NMDAR) and L-type Ca^{2+} channels to the observed Ca^{2+} signals and to simplify the analysis, the imaging experiments were performed in Ca^{2+}-free media containing 100 μM EGTA (see Experimental Procedures for details). The local Ca^{2+} concentration in these experiments is estimated from the ratio of Fura-2 signals at 340 nm and 380 nm excitation wavelengths as shown by pseudocolor images. Representative data with EGFP, EGFP + Htt-23Q, EGFP + Htt-82Q, and EGFP + Htt-138Q transfected MSN neurons are shown on Figure 6. The transfected cells were identified by GFP imaging (Figure 6, first column, arrows) prior to collecting quantitative Fura-2 340/380 ratio data. We noticed that prior to application of DHPG, the basal Ca^{2+} levels were slightly elevated in Htt-transfected cells when compared to control cells (Figure 6, second column). On average, the basal 340/380 ratio was equal to 0.43 ± 0.02 (n = 14) for EGFP-transfected cells (Figures 7A and 7I), 0.51 ± 0.02 (n = 18) for EGFP + Htt-23Q, 0.55 ± 0.02 (n = 29) for EGFP + Htt-82Q, and 0.54 ± 0.015 (n = 21) for EGFP + Htt-138Q (Figures 7C, 7E, 7G, and 7I). The basal Ca^{2+} levels were significantly ($p < 0.01$, unpaired t test) higher in Htt-transfected MSNs as compared to control MSNs. These results are in agreement with elevated basal Ca^{2+} levels observed in hippocampal neurons from YAC46 transgenic HD mice (Hodgson et al., 1999).

Ten micromolar DHPG corresponds to a threshold concentration for mGluR1/5 receptor activation in MSN neurons, and only a small response to DHPG application at this concentration was observed in control MSNs transfected with EGFP plasmid alone (Figure 6, first row, and Figures 7A and 7B) and in MSN neurons transfected with Htt-23Q plasmid (Figure 6, second row, and Figures 7C and 7D). In contrast, significant response to 10 μM DHPG was observed in MSNs transfected with Htt-82Q plasmid (Figure 6, third row, and Figures 7E and 7F). Even stronger response to this agonist was observed in MSNs transfected with Htt-138Q plasmid (Figure 6, fourth row, and Figures 7G and 7H). Paired t test analysis revealed that peak 340/380 ratios were significantly ($p < 0.001$) higher than basal 340/380 ratios in Htt-82Q and Htt-138Q transfected neurons, but not in Htt-23Q and EGFP-only transfected neurons (Figure 7I). Thus, we concluded that overexpression of full-length Htt^{exp} sensitizes $InsP_3R1$ to $InsP_3$ in MSN neurons. The effects of Htt^{exp} on $InsP_3R1$ function were most pronounced at threshold levels of stimulation, as control, Htt-, and Htt^{exp}-transfected MSN neurons responded in a similar manner to 500 μM DHPG (data not shown).

Htt is a substrate for cleavage by caspases, and Htt proteolysis may be an early step in the pathogenesis of HD (Wellington et al., 2000, 2002). Removal of caspase 3 and 6 cleavage sites in the Htt quintuple caspase-resistant mutants [Htt(R)] reduces Htt^{exp} proteolysis and toxicity in apoptotically stressed neurons (Wellington et al., 2000). Does sensitization of $InsP_3R1$ by Htt^{exp} depend on prior cleavage by caspases? To answer this question, we cotransfected MSN neurons with EGFP + Htt(R)-15Q or EGFP + Htt(R)-138Q and analyzed responses of transfected cells to 10 μM DHPG. We discovered that Htt(R)-138Q, but not Htt(R)-15Q, significantly potentiated DHPG-induced Ca^{2+} release in MSNs (Figure 7I). Importantly, the potentiating effects of caspase-resistant Htt(R)-138Q and the cleavable form of Htt-138Q were similar (Figure 7I). From these results, we concluded that Htt^{exp}

does not require proteolytic cleavage by caspases 3 and 6 to have potentiating effects on $InsP_3R1$-mediated Ca^{2+} release in MSN neurons.

Discussion

Huntington's Disease and Abnormal Ca^{2+} Signaling

Programmed neuronal death (apoptosis) underlies the symptoms of many neurodegenerative disorders, including Alzheimer's, Parkinson's, and Huntington's disease (Mattson, 2000). Ca^{2+} plays an important role in neuronal signaling (Berridge, 1998), and perturbed Ca^{2+} homeostasis is one of the key steps during initiation of the apoptotic program in affected neurons (Mattson and Chan, 2001). Abnormalities in ER-mediated Ca^{2+} signaling due to a mutation of presenilin 1 have been linked to the development of Alzheimer's disease (Mattson and Chan, 2001). Several lines of experimental evidence point to a connection between HD and aberrant neuronal Ca^{2+} signaling. Abnormally high cytosolic Ca^{2+} levels were detected in CA1 pyramidal neurons from the YAC46 HD mouse model (Hodgson et al., 1999). The lymphoblast mitochondria of HD human patients and brain mitochondria from the YAC72 HD mouse model display abnormal Ca^{2+} homeostasis (Panov et al., 2002). The derangement in Ca^{2+} signaling occurs early (Panov et al., 2002) and can therefore be invoked as an initiating event in the pathogenesis of HD, followed by activation of caspases in response to high Ca^{2+} levels (Juin et al., 1998; Zeron et al., 2002). In addition to promoting apoptosis, increased caspase activity would be expected to catalyze Htt^{exp} proteolysis (Wellington et al., 2002), resulting in the generation of toxic amino-terminal Htt^{exp} fragments (Hackam et al., 1998). Abnormally high Ca^{2+} levels would also be expected to promote Htt^{exp} proteolysis via calpain-dependent mechanisms (Goffredo et al., 2002; Kim et al., 2001).

What are the molecular mechanisms linking the Htt^{exp} mutation with increased Ca^{2+} levels in affected neurons? Htt^{exp} alters mitochondrial Ca^{2+} homeostasis by directly interacting with the mitochondrial membrane (Panov et al., 2002). While this interaction likely contributes to mitochondrial dysfunction, it remains unclear how intracellular Ca^{2+} is affected by Htt^{exp} at the mitochondria. An alternative molecular mechanism has been suggested by the recent description of a Htt-PSD95-NMDAR complex (Sun et al., 2001) and the ability of Htt^{exp} to potentiate NMDAR function (Chen et al., 1999; Sun et al., 2001; Zeron et al., 2002). In addition to influx via NMDAR and voltage-gated Ca^{2+} channels, neuronal Ca^{2+} is also largely influenced by release from intracellular stores in the endoplasmic reticulum (ER) upon activation of class 1 metabotropic glutamate receptors (mGluR1/5) (Pin and Duvoisin, 1995). The alterations in ER enzymes that have been observed in HD brains (Cross et al., 1985) might be caused by abnormal Ca^{2+} release from the ER (Korkotian et al., 1999). Here, we describe a novel mechanism linking Htt^{exp} to $InsP_3R1$-mediated Ca^{2+} release from the ER in striatal MSNs.

$InsP_3R1$-HAP1A-Htt Functional Complex

We have identified a protein complex that contains $InsP_3R1$, Htt, and HAP1. This complex was discovered through the identification of HAP1A as a binding partner of the $InsP_3R1$ cytosolic carboxy-terminal tail in the Y2H screen (Figures 1A and 1B). In biochemical experiments, we found that Htt directly interacts with the $InsP_3R1$ cytosolic carboxy-terminal tail and that binding to this limited region of $InsP_3R1$ was highly dependent on both the presence of HAP1A and polyQ expansion within Htt (Figure 1E). Htt also binds to full-length $InsP_3R1$, but this interaction is not strongly modulated by polyQ expansion (Figures 3A and 5A) or the presence of HAP1A (Figures 2C, 3A, and 5A).

The effects of Htt and HAP1A on $InsP_3R1$ function are largely consistent with our biochemical analysis. In planar lipid bilayer experiments, the Htt^{exp} amino terminus or full-length Htt^{exp}, but not wild-type Htt, greatly facilitated $InsP_3R1$ activity at 100 nM $InsP_3$ (Figures 3B, 3C, 5D, and 5E). However, the amino terminus of wild-type Htt facilitated $InsP_3R1$ activity in the presence of HAP1A (Figures 4A and 4B). Thus, $InsP_3R1$ is sensitized to $InsP_3$ in conditions when Htt binds to the $InsP_3R1$ carboxy terminus (Htt^{exp} or Htt with HAP1A), but not in conditions when Htt does not bind to $InsP_3R1$ carboxy terminus (Htt alone). From these results we concluded that association of Htt^{exp} or Htt-HAP1A with $InsP_3R1$ carboxy terminus sensitizes $InsP_3R1$ to activation by $InsP_3$.

Sensitization of $InsP_3R1$ and NMDAR by Htt^{exp} and Huntington's Disease

The molecular and cellular basis for selective vulnerability of MSNs in HD remains elusive. One proposed mechanism is centered on the finding that MSNs primarily express the NR1A/NR2B subtype of NMDAR (Kuppenbender et al., 1999; Landwehrmeyer et al., 1995; Zeron et al., 2002). Importantly, Htt^{exp} appears to selectively enhance the activity of NR1A/NR2B channels, relative to other NMDAR subtypes, suggesting that increased NMDAR function might be specifically occurring in MSNs of HD patients (Chen et al., 1999; Sun et al., 2001; Zeron et al., 2001). Our results suggest another possible explanation for selectivity in HD involving the enrichment of mGluR5, a member of the group I mGluRs, in MSNs (Kerner et al., 1997; Mao and Wang, 2001, 2002; Tallaksen-Greene et al., 1998). Stimulation of group I mGluR in MSNs leads to the generation of $InsP_3$ and release of Ca^{2+} via $InsP_3R1$ (Mao and Wang, 2002). In addition, stimulation of group I mGluR is known to potentiate NMDAR activity in neurons, most likely via a PKC-dependent pathway (Calabresi et al., 1999; Pisani et al., 2001; Skeberdis et al., 2001).

In striatal MSNs, the presence of full-length Htt^{exp} sensitizes Ca^{2+} release in response to subthreshold concentrations of the mGluR1/5 agonist DHPG (Figures 6 and 7). We propose that sensitizing influences of Htt^{exp} on $InsP_3R1$ and the NR1A/NR2B subtype of NMDAR (Chen et al., 1999; Sun et al., 2001; Zeron et al., 2001) have a synergistic effect on glutamate-induced Ca^{2+} signals in MSNs of HD individuals (Figure 8). In MSNs of HD patients, the activation of both mGluR5 and NMDAR by low concentrations of glutamate released by corticostriatal projection neurons leads to supranormal Ca^{2+} signals (Figure 8B) when compared to normal MSNs (Figure 8A), resulting in neuronal dysfunction and apoptosis. Overall, our findings provide support for the hypothesis that perturbation of neuronal Ca^{2+} signaling mediated by NMDAR and $InsP_3R1$ may be a primary cause of MSN selectivity in HD. In our model, the toxic "gain of Htt^{exp} function" (Tobin and Signer, 2000) corresponds to the polyQ-dependent ability of Htt^{exp} to sensitize NMDAR and $InsP_3R1$-mediated Ca^{2+} signals in MSN neurons (Figure 8B). In addition, our model points to mGluR5 as potential target for pharmacological treatment of HD.

Experimental Procedures

Yeast Two-Hybrid Methods

The carboxy-terminal region of rat $InsP_3R1$ (Mignery et al., 1990) (amino acids D2590–A2749) was amplified by PCR and cloned into pLexN vector (IC bait). The yeast two-hybrid screen of a rat brain (P8-P9) cDNA library (kind gift of Dr. T. Südhof) with the IC bait and liquid yeast two-hybrid assays were performed as previously described (Maximov et al., 2003).

Plasmids

The following rat $InsP_3R1$ (Mignery et al., 1990) baits in pLexN vectotor were generated by PCR (listed by encoded amino acid and residue numbers): IC = D2590–A2749, IC_G2736X

= D2590–G2736, IC3 = R2676–A2749, IC4 = Q2714–A2749, IC5 = D2590–Q2714, IC6 = D2590–R2676, IC7 = D2590–L2646, IC8 = D2590–F2627, IC9 = L2646–A2749, IC10 = F2627–A2749. The $InsP_3R1$ expression constructs in pGEX-KG are GST-IC8 = D2590–F2627 and GST-IC10 = F2627–A2749. The full-length clones of rat HAP1A and HAP1B (Li et al., 1995) were amplified by RT-PCR from rat brain mRNA and cloned into the pVp16-3 yeast two-hybrid prey vector, pCMV-HA mammalian expression vector, and pGEX-KG bacterial expression vector. Full-length Htt plasmids Htt-23Q (HD-FL-23Q) and Htt-82Q (HD-FL-82Q) in pRc/CMV expression vector were kindly provided by Dr. Christopher A Ross (Cooper et al., 1998). The full-length Htt-15Q and Htt-138Q plasmids (Wellington et al., 2000) were cloned into the pCI expression vector (Promega). The caspase 3 and 6 resistant Htt quintuple mutant plasmids Htt(R)-15Q and Htt(R)-138Q in pRc/CMV vector have been previously described (Wellington et al., 2000). The Htt-N expression constructs in pGEX-KG are Htt-N-15Q/138Q = M1–K158 of human Htt.

GST Pull-Down Assays

GST-IC8 and GST-IC10 proteins were expressed in the BL21 *E. coli* strain and purified on glutathione-agarose beads. HA-HAP1A and HA-HAP1B were expressed in COS7 cells by DEAE-dextran transfection (Sambrook et al., 1989). Htt-23/82Q proteins were expressed in HEK293 cells by calcium-phosphate transfection (Sambrook et al., 1989). 48 hr after transfection, COS7 or HEK293 cells were collected with ice-cold PBS and solubilized for 30 min at 4°C in extraction buffer A (1% CHAPS, 137 mM NaCl, 2.7 mM KCl, 4.3 mM Na_2HPO_4, 1.4 mM KH_2PO_4 [pH 7.2], 5 mM EDTA, 5 mM EGTA, and protease inhibitors). Extracts were clarified by centrifugation for 20 min at 100,000 × g and incubated for 1 hr at 4°C with GST-IC8 or GST-IC10 proteins. Beads were washed three times with the extraction buffer A. Attached proteins were analyzed by Western blotting with anti-Htt or anti-HA monoclonal antibodies.

In Vitro Binding Assay

Full-length rat $InsP_3R1$ (RT1)-encoding baculoviruses were previously described (Tu et al., 2002). Full-length Htt plasmids Htt-23Q and Htt-82Q (Cooper et al., 1998) were subcloned into pFastBac1 vector (Invitrogen), and Htt-23Q/82Q baculoviruses were generated using Bac-to-Bac system (Invitrogen). The *Spodoptera frugiperda* (Sf9) cells (100 ml) were infected with RT1 viruses or coinfected with RT1:Htt-23Q/82Q viral mixtures (3:1) and collected by centrifugation 72 hr postinfection. The RT1-infected cells were solubilized in extraction buffer A, cleared by centrifugation (100,000 × g), and mixed with an equal volume of HA-HAP1A or HA-HAP1B-expressing COS7 lystates prepared as described above for 2 hr at 4°C. The mixture was precipitated with anti-$InsP_3R1$ polyclonal antibody (T443) attached to protein A-Sepharose beads and analyzed by Western blotting with anti-HA monoclonal antibodies. The cells coinfected with RT1 and Htt-23Q/82Q baculoviruses were used to prepare microsomes for bilayer experiments as previously described (Tu et al., 2002). Obtained microsomes were solubilized in extraction buffer A, cleared by centrifugation (100,000 × g in TL-100), used in immunoprecipitation experiments with anti-$InsP_3R1$ polyclonal antibodies, and analyzed by Western blotting with anti-Htt monoclonal antibodies.

Brain Pull-Downs and Immunoprecipitations

Rat and mouse brain tissues were isolated, homogenized, and solubilized for 1.5 hr at 4°C in extraction buffer A. The lysate was clarified by 20 min centrifugation at 100,000 × g and utilized in pull-down experiments with GST-IC8 and GST-IC10 proteins or in the immunoprecipitation experiments with anti-$InsP_3R1$ polyclonal antibodies (T443) performed as described above. GST-IC8 and GST-IC10 proteins (200 μg/ml final concentration) were included in the immunoprecipitation reactions as indicated. An

additional 0.5 M KCl wash step was included in the immunoprecipitation experiments with mouse samples as indicated in the text. The precipitated fractions were analyzed by Western blotting with anti-Htt and anti-HAP1 monoclonal antibodies.

Planar Lipid Bilayer Experiments

Single-channel recordings of recombinant $InsP_3R1$ (RT1) expressed in isolation or coexpressed with Htt-23Q/82Q proteins were performed as previously described (Tang et al., 2003; Tu et al., 2002) at 0 mV transmembrane potential using 50 mM Ba^{2+} (*trans*) as a charge carrier. The *cis* (cytosolic) chamber contained 110 mM Tris dissolved in HEPES (pH 7.35), 0.5 mM Na_2ATP, pCa 6.7 (0.2 mM EGTA + 0.14 mM $CaCl_2$) (Bezprozvanny et al., 1991). $InsP_3R1$ were activated by addition of 100 nM $InsP_3$ or 2 μM $InsP_3$ (Alexis) to the *cis* chamber as indicated in the text. GST, Htt-N-15Q, Htt-N-138Q, and HAP1A proteins were expressed in *BL21 E. coli*, purified on gluthathione beads, eluted with reduced glutathione, dialyzed overnight against *cis* recording buffer (110 mM Tris/HEPES [pH 7.35]), and added in 1 μl volume (0.3 mg/ml protein with addition of 0.02 mM ruthenium red) directly to the *cis* side of the bilayer containing $InsP_3R1$ without stirring. Exposure of $InsP_3R1$ to the test proteins was terminated 2–3 min after addition by stirring the *cis* chamber for 30 s (1:3000 dilution of test protein stocks). The $InsP_3R1$ single-channel currents were amplified (Warner OC-725), filtered at 1 kHz by a low-pass eight-pole Bessel filter, digitized at 5 kHz (Digidata 1200, Axon Instruments), and stored on computer hard drive and recordable optical discs. For off-line computer analysis (pClamp 6, Axon Instruments), currents were filtered digitally at 500 Hz. For presentation of the current traces, data were filtered at 200 Hz.

Ca^{2+} Imaging Experiments

The rat medium spiny neuronal (MSN) cultures on poly-D-lysine (Sigma) coated 12 mm round glass coverslips were established by following published procedures (Mao and Wang, 2001). The 5 μM of cytosine arabinoside (AraC, Sigma) was added at 2–4 DIV to inhibit glial cell growth. At 20 DIV the MSN cultures were transfected by the calcium-phosphate method (Maximov and Bezprozvanny, 2002) with EGFP-C3 plasmid (Clontech) or a 1:3 mixture of EGFP:Htt plasmids as indicated in the text. 48 hr after transfection, the MSN neurons were loaded with 5 μM Fura2-AM (Molecular Probes) in artificial cerebrospinal fluid (ACSF) (140 mM NaCl, 5 mM KCl, 1 mM $MgCl_2$, 2 mM $CaCl_2$, 10 mM HEPES [pH 7.3]) for 45 min at 37°C. For imaging experiments the coverslips were mounted onto a recording/perfusion chamber (RC-26G, Warner Instrument) maintained at 37°C (PH1, Warner Instrument), positioned on the movable stage of an Olympus IX-70 inverted microscope, and perfused with ACSF media by gravity flow. Following GFP imaging, the coverslip was washed extensively with Ca^{2+}-free ACSF (omitted $CaCl_2$ from ACSF and supplemented with 100 μM EGTA). In Ca^{2+} imaging experiments the MSN cells were intermittently excited by 340 nm and 380 nm UV light (DeltaRAM illuminator, PTI) using a Fura-2 dichroic filter cube (Chroma Technologies) and 60× UV-grade oil-immersed objective (Olympus). The emitted light was collected by an IC-300 camera (PTI), and the images were digitized by ImageMaster Pro software (PTI). Baseline (6 min) measurements were obtained prior to bath application of 10 μM or 500 μM 3,5-DHPG (Tocris) dissolved in Ca^{2+}-free ACSF. The DHPG solutions were prewarmed to 37°C before application to MSNs. Images at 340 and 380 nm excitation wavelengths were captured every 5 s and shown as 340/380 image ratios at time points as indicated. Background fluorescence was determined according to manufacturer's (PTI) recommendations and subtracted.

Antibodies

The following monoclonal antibodies were used: anti-HA (HA.11) from Covance, anti-Htt (mAB2166) from Chemicon International, Intramonoclonal anti-HAP1 1B6 is a kind gift of

Dr. Claire-Anne Gutekunst (Chan et al., 2002), GAD65 antibodies from BD Pharmingen. Polyclonal anti-InsP_3R1 T443 antibody was previously described (Kaznacheyeva et al., 1998). Secondary HRP-conjugated anti-rabbit and anti-mouse antibodies were from Jackson Imunoresearch.

Acknowledgments

We thank Thomas C. Südhof for advice with yeast two-hybrid screen and the gift of a rat brain cDNA library and Phyllis Foley for administrative assistance. We thank Thomas C. Südhof for rat InsP_3R1 cDNA, Claire-Anne Gutekunst for HAP1 monoclonal antibodies, and Christopher A Ross for HD-FL-23Q and HD-FL-82Q plasmids. I.B. is supported by the Robert A. Welch Foundation, the Huntington's Disease Society of America, the Hereditary Disease Foundation, and NIH R01 NS38082. M.R.H. is supported by the Canadian Institutes of Health Research, the Hereditary Disease Foundation, and the Huntington's Disease Society of America and holds a Canada Research Chair in Human Genetics.

References

Berridge MJ. Neuronal calcium signaling. Neuron. 1998; 21:13–26. [PubMed: 9697848]

Bertaux F, Sharp AH, Ross CA, Lehrach H, Bates GP, Wanker E. HAP1-huntingtin interactions do not contribute to the molecular pathology in Huntington's disease transgenic mice. FEBS Lett. 1998; 426:229–232. [PubMed: 9599014]

Bezprozvanny I, Watras J, Ehrlich BE. Bell-shaped calcium-response curves of Ins(1,4,5)P_3- and calcium-gated channels from endoplasmic reticulum of cerebellum. Nature. 1991; 351:751–754. [PubMed: 1648178]

Calabresi P, Centonze D, Pisani A, Bernardi G. Metabotropic glutamate receptors and cell-type-specific vulnerability the striatum: implication for ischemia and Huntington's disease. Exp. Neurol. 1999; 158:97–108. [PubMed: 10448421]

Chan EY, Nasir J, Gutekunst CA, Coleman S, Maclean A, Maas A, Metzler M, Gertsenstein M, Ross CA, Nagy A, Hayden MR. Targeted disruption of Huntingtin-associated protein-1 (Hap1) results in postnatal death due to depressed feeding behavior. Hum. Mol. Genet. 2002; 11:945–959. [PubMed: 11971876]

Chen N, Luo T, Wellington C, Metzler M, McCutcheon K, Hayden MR, Raymond LA. Subtype-specific enhancement of NMDA receptor currents by mutant huntingtin. J. Neurochem. 1999; 72:1890–1898. [PubMed: 10217265]

Chesselet MF, Mercugliano M, Soghomonian JJ, Salin P, Qin Y, Gonzales C. Regulation of glutamic acid decarboxylase gene expression in efferent neurons of the basal ganglia. Prog. Brain Res. 1993; 99:143–154. [PubMed: 8108545]

Colomer V, Engelender S, Sharp AH, Duan K, Cooper JK, Lanahan A, Lyford G, Worley P, Ross CA. Huntingtin-associated protein 1 (HAP1) binds to a Trio-like polypeptide, with a rac1 guanine nucleotide exchange factor domain. Hum. Mol. Genet. 1997; 6:1519–1525. [PubMed: 9285789]

Cooper JK, Schilling G, Peters MF, Herring WJ, Sharp AH, Kaminsky Z, Masone J, Khan FA, Delanoy M, Borchelt DR, et al. Truncated N-terminal fragments of huntingtin with expanded glutamine repeats form nuclear and cytoplasmic aggregates in cell culture. Hum. Mol. Genet. 1998; 7:783–790. [PubMed: 9536081]

Cross AJ, Crow TJ, Johnson JA, Dawson JM, Peters TJ. Loss of endoplasmic reticulum-associated enzymes affected brain regions in Huntington's disease and Alzheimer-type dementia. J. Neurol. Sci. 1985; 71:137–143. [PubMed: 2935594]

Engelender S, Sharp AH, Colomer V, Tokito MK, Flanagan A, Worley P, Holzbaur EL, Ross CA. Huntingtin-associated protein 1 (HAP1) interacts with the p150Glued subunit of dynactin. Hum. Mol. Genet. 1997; 6:2205–2212. [PubMed: 9361024]

Furuichi T, Kohda K, Miyawaki A, Mikoshiba K. Intra-cellular channels. Curr. Opin. Neurobiol. 1994; 4:294–303. [PubMed: 7522674]

Gerfen CR. The neostriatal mosaic: multiple levels of compartmental organization. Trends Neurosci. 1992; 15:133–139. [PubMed: 1374971]

Goffredo D, Rigamonti D, Tartari M, De Micheli A, Verderio C, Matteoli M, Zuccato C, Cattaneo E. Calcium-dependent cleavage of endogenous wild-type huntingtin in primary cortical neurons. J. Biol. Chem. 2002; 277:39594–39598. [PubMed: 12200414]

Gusella JF, MacDonald ME. Huntingtin: a single bait hooks many species. Curr. Opin. Neurobiol. 1998; 8:425–430. [PubMed: 9687360]

Gutekunst CA, Li SH, Yi H, Ferrante RJ, Li XJ, Hersch SM. The cellular and subcellular localization of huntingtin-associated protein 1 (HAP1): comparison with huntingtin in rat and human. J. Neurosci. 1998; 18:7674–7686. [PubMed: 9742138]

Hackam AS, Singaraja R, Wellington CL, Metzler M, McCutcheon K, Zhang T, Kalchman M, Hayden MR. The influence of huntingtin protein size on nuclear localization and cellular toxicity. J. Cell Biol. 1998; 141:1097–1105. [PubMed: 9606203]

HDCRG (The Huntington's Disease Collaborative Research Group). A novel gene containing a trinucleotide repeat that is expanded and unstable on Huntington's disease chromosomes. Cell. 1993; 72:971–983. [PubMed: 8458085]

Hodgson JG, Agopyan N, Gutekunst CA, Leavitt BR, LePiane F, Singaraja R, Smith DJ, Bissada N, McCutcheon K, Nasir J, et al. A YAC mouse model for Huntington's disease with full-length mutant huntingtin, cytoplasmic toxicity, and selective striatal neurodegeneration. Neuron. 1999; 23:181–192. [PubMed: 10402204]

Juin P, Pelletier M, Oliver L, Tremblais K, Gregoire M, Meflah K, Vallette FM. Induction of a caspase-3-like activity by calcium in normal cytosolic extracts triggers nuclear apoptosis in a cell-free system. J. Biol. Chem. 1998; 273:17559–17564. [PubMed: 9651349]

Kalchman MA, Koide HB, McCutcheon K, Graham RK, Nichol K, Nishiyama K, Kazemi-Esfarjani P, Lynn FC, Wellington C, Metzler M, et al. HIP1, a human homologue of S. cerevisiae Sla2p, interacts with membrane-associated huntingtin in the brain. Nat. Genet. 1997; 16:44–53. [PubMed: 9140394]

Kaznacheyeva E, Lupu VD, Bezprozvanny I. Single-channel properties of inositol (1,4,5)-trisphosphate receptor heterologously expressed in HEK-293 cells. J. Gen. Physiol. 1998; 111:847–856. [PubMed: 9607940]

Kerner JA, Standaert DG, Penney JB Jr, Young AB, Landwehrmeyer GB. Expression of group one metabotropic glutamate receptor subunit mRNAs in neurochemically identified neurons in the rat neostriatum, neocortex, and hippocampus. Brain Res. Mol. Brain Res. 1997; 48:259–269. [PubMed: 9332723]

Kim YJ, Yi Y, Sapp E, Wang Y, Cuiffo B, Kegel KB, Qin ZH, Aronin N, DiFiglia M. Caspase 3-cleaved N-terminal fragments of wild-type and mutant huntingtin are present in normal and Huntington's disease brains, associate with membranes, and undergo calpain-dependent proteolysis. Proc. Natl. Acad. Sci. USA. 2001; 98:12784–12789. [PubMed: 11675509]

Korkotian E, Schwarz A, Pelled D, Schwarzmann G, Segal M, Futerman AH. Elevation of intracellular glucosylceramide levels results in an increase in endoplasmic reticulum density and in functional calcium stores in cultured neurons. J. Biol. Chem. 1999; 274:21673–21678. [PubMed: 10419477]

Kuppenbender KD, Albers DS, Iadarola MJ, Landwehrmeyer GB, Standaert DG. Localization of alternatively spliced NMDAR1 glutamate receptor isoforms in rat striatal neurons. J. Comp. Neurol. 1999; 415:204–217. [PubMed: 10545160]

Landwehrmeyer GB, Standaert DG, Testa CM, Penney JB Jr, Young AB. NMDA receptor subunit mRNA expression by projection neurons and interneurons in rat striatum. J. Neurosci. 1995; 15:5297–5307. [PubMed: 7623152]

Li XJ, Li SH, Sharp AH, Nucifora FC Jr, Schilling G, Lanahan A, Worley P, Snyder SH, Ross CA. A huntingtin-associated protein enriched in brain with implications for pathology. Nature. 1995; 378:398–402. [PubMed: 7477378]

Li SH, Gutekunst CA, Hersch SM, Li XJ. Interaction of huntingtin-associated protein with dynactin P150Glued. J. Neurosci. 1998a; 18:1261–1269. [PubMed: 9454836]

Li SH, Hosseini SH, Gutekunst CA, Hersch SM, Ferrante RJ, Li XJ. A human HAP1 homologue. Cloning, expression, and interaction with huntingtin. J. Biol. Chem. 1998b; 273:19220–19227. [PubMed: 9668110]

Li Y, Chin LS, Levey AI, Li L. Huntingtin-associated protein 1 interacts with hepatocyte growth factor-regulated tyrosine kinase substrate and functions in endosomal trafficking. J. Biol. Chem. 2002; 277:28212–28221. [PubMed: 12021262]

Mao L, Wang JQ. Upregulation of preprodynorphin and preproenkephalin mRNA expression by selective activation of group I metabotropic glutamate receptors in characterized primary cultures of rat striatal neurons. Brain Res. Mol. Brain Res. 2001; 86:125–137. [PubMed: 11165379]

Mao L, Wang JQ. Glutamate cascade to cAMP response element-binding protein phosphorylation in cultured striatal neurons through calcium-coupled group I metabotropic glutamate receptors. Mol. Pharmacol. 2002; 62:473–484. [PubMed: 12181423]

Matsumoto M, Nakagawa T, Inoue T, Nagata E, Tanaka K, Takano H, Minowa O, Kuno J, Sakakibara S, Yamada M, et al. Ataxia and epileptic seizures in mice lacking type 1 inositol 1,4,5-trisphosphate receptor. Nature. 1996; 379:168–171. [PubMed: 8538767]

Mattson MP. Apoptosis in neurodegenerative disorders. Nat. Rev. Mol. Cell Biol. 2000; 1:120–129. [PubMed: 11253364]

Mattson MP, Chan SL. Dysregulation of cellular calcium homeostasis in Alzheimer's disease: bad genes and bad habits. J. Mol. Neurosci. 2001; 17:205–224. [PubMed: 11816794]

Maximov A, Bezprozvanny I. Synaptic targeting of N-type calcium channels in hippocampal neurons. J. Neurosci. 2002; 22:6939–6952. [PubMed: 12177192]

Maximov A, Tang T-S, Bezprozvanny I. Association of the type 1 inositol (1,4,5)-trisphosphate receptor with 4.1N protein in neurons. Mol. Cell. Neurosci. 2003; 22:271–283. [PubMed: 12676536]

Menalled LB, Chesselet MF. Mouse models of Huntington's disease. Trends Pharmacol. Sci. 2002; 23:32–39. [PubMed: 11804649]

Mignery GA, Newton CL, Archer BT, Sudhof TC. Structure and expression of the rat inositol 1,4,5-trisphosphate receptor. J. Biol. Chem. 1990; 265:12679–12685. [PubMed: 2165071]

Nasir J, Goldberg YP, Hayden MR. Huntington disease: new insights into the relationship between CAG expansion and disease. Hum. Mol. Genet. 1996; 5:1431–1435. [PubMed: 8875248]

Nasir J, Duan K, Nichol K, Engelender S, Ashworth R, Colomer V, Thomas S, Disteche CM, Hayden MR, Ross CA. Gene structure and map location of the murine homolog of the Huntington-associated protein, Hap1. Mamm. Genome. 1998; 9:565–570. [PubMed: 9657855]

Page KJ, Potter L, Aronni S, Everitt BJ, Dunnett SB. The expression of Huntingtin-associated protein (HAP1) mRNA in developing, adult and ageing rat CNS: implications for Huntington's disease neuropathology. Eur. J. Neurosci. 1998; 10:1835–1845. [PubMed: 9751154]

Panov AV, Gutekunst CA, Leavitt BR, Hayden MR, Burke JR, Strittmatter WJ, Greenamyre JT. Early mitochondrial calcium defects in Huntington's disease are a direct effect of polyglutamines. Nat. Neurosci. 2002; 5:731–736. [PubMed: 12089530]

Pin JP, Duvoisin R. The metabotropic glutamate receptors: structure and functions. Neuropharmacology. 1995; 34:1–26. [PubMed: 7623957]

Pisani A, Gubellini P, Bonsi P, Conquet F, Picconi B, Centonze D, Bernardi G, Calabresi P. Metabotropic glutamate receptor 5 mediates the potentiation of N-methyl-D-aspartate responses in medium spiny striatal neurons. Neuroscience. 2001; 106:579–587. [PubMed: 11591458]

Rubinsztein DC. Lessons from animal models of Huntington's disease. Trends Genet. 2002; 18:202–209. [PubMed: 11932021]

Sambrook, J.; Fritsch, EF.; Maniatis, T. Molecular Cloning: A Laboratory Manual. 2nd Edition. New York: Cold Spring Harbor Laboratory Press; 1989.

Schoepp DD, Jane DE, Monn JA. Pharmacological agents acting at subtypes of metabotropic glutamate receptors. Neuropharmacology. 1999; 38:1431–1476. [PubMed: 10530808]

Singaraja RR, Hadano S, Metzler M, Givan S, Wellington CL, Warby S, Yanai A, Gutekunst CA, Leavitt BR, Yi H, et al. HIP14, a novel ankyrin domain-containing protein, links huntingtin to intracellular trafficking and endocytosis. Hum. Mol. Genet. 2002; 11:2815–2828. [PubMed: 12393793]

Skeberdis VA, Lan J, Opitz T, Zheng X, Bennett MV, Zukin RS. mGluR1-mediated potentiation of NMDA receptors involves a rise in intracellular calcium and activation of protein kinase C. Neuropharmacology. 2001; 40:856–865. [PubMed: 11378156]

Street VA, Bosma MM, Demas VP, Regan MR, Lin DD, Robinson LC, Agnew WS, Tempel BL. The type 1 inositol 1,4,5-trisphosphate receptor gene is altered in the opisthotonos mouse. J. Neurosci. 1997; 17:635–645. [PubMed: 8987786]

Sun Y, Savanenin A, Reddy PH, Liu YF. Polyglutamine-expanded huntingtin promotes sensitization of N-methyl-D-aspartate receptors via post-synaptic density 95. J. Biol. Chem. 2001; 276:24713–24718. [PubMed: 11319238]

Tallaksen-Greene SJ, Kaatz KW, Romano C, Albin RL. Localization of mGluR1a-like immunoreactivity and mGluR5-like immunoreactivity in identified populations of striatal neurons. Brain Res. 1998; 780:210–217. [PubMed: 9507137]

Tang TS, Tu H, Wang Z, Bezprozvanny I. Modulation of type 1 inositol (1,4,5)-trisphosphate receptor function by protein kinase a and protein phosphatase 1alpha. J. Neurosci. 2003; 23:403–415. [PubMed: 12533600]

Tobin AJ, Signer ER. Huntington's disease: the challenge for cell biologists. Trends Cell Biol. 2000; 10:531–536. [PubMed: 11121745]

Tu H, Miyakawa T, Wang Z, Glouchankova L, Iino M, Bezprozvanny I. Functional characterization of the type 1 inositol 1,4,5-trisphosphate receptor coupling domain SII(+/−) splice variants and the *opisthotonos* mutant form. Biophys. J. 2002; 82:1995–2004. [PubMed: 11916857]

Vonsattel JP, DiFiglia M. Huntington disease. J. Neuropathol. Exp. Neurol. 1998; 57:369–384. [PubMed: 9596408]

Vonsattel JP, Myers RH, Stevens TJ, Ferrante RJ, Bird ED, Richardson EP Jr. Neuropathological classification of Huntington's disease. J. Neuropathol. Exp. Neurol. 1985; 44:559–577. [PubMed: 2932539]

Wellington CL, Singaraja R, Ellerby L, Savill J, Roy S, Leavitt B, Cattaneo E, Hackam A, Sharp A, Thornberry N, et al. Inhibiting caspase cleavage of huntingtin reduces toxicity and aggregate formation in neuronal and nonneuronal cells. J. Biol. Chem. 2000; 275:19831–19838. [PubMed: 10770929]

Wellington CL, Ellerby LM, Gutekunst CA, Rogers D, Warby S, Graham RK, Loubser O, van Raamsdonk J, Singaraja R, Yang YZ, et al. Caspase cleavage of mutant huntingtin precedes neurodegeneration in Huntington's disease. J. Neurosci. 2002; 22:7862–7872. [PubMed: 12223539]

Zeron MM, Chen N, Moshaver A, Lee AT, Wellington CL, Hayden MR, Raymond LA. Mutant huntingtin enhances excitotoxic cell death. Mol. Cell. Neurosci. 2001; 17:41–53. [PubMed: 11161468]

Zeron MM, Hansson O, Chen N, Wellington CL, Leavitt BR, Brundin P, Hayden MR, Raymond LA. Increased sensitivity to N-methyl-D-aspartate receptor-mediated excitotoxicity in a mouse model of Huntington's disease. Neuron. 2002; 33:849–860. [PubMed: 11906693]

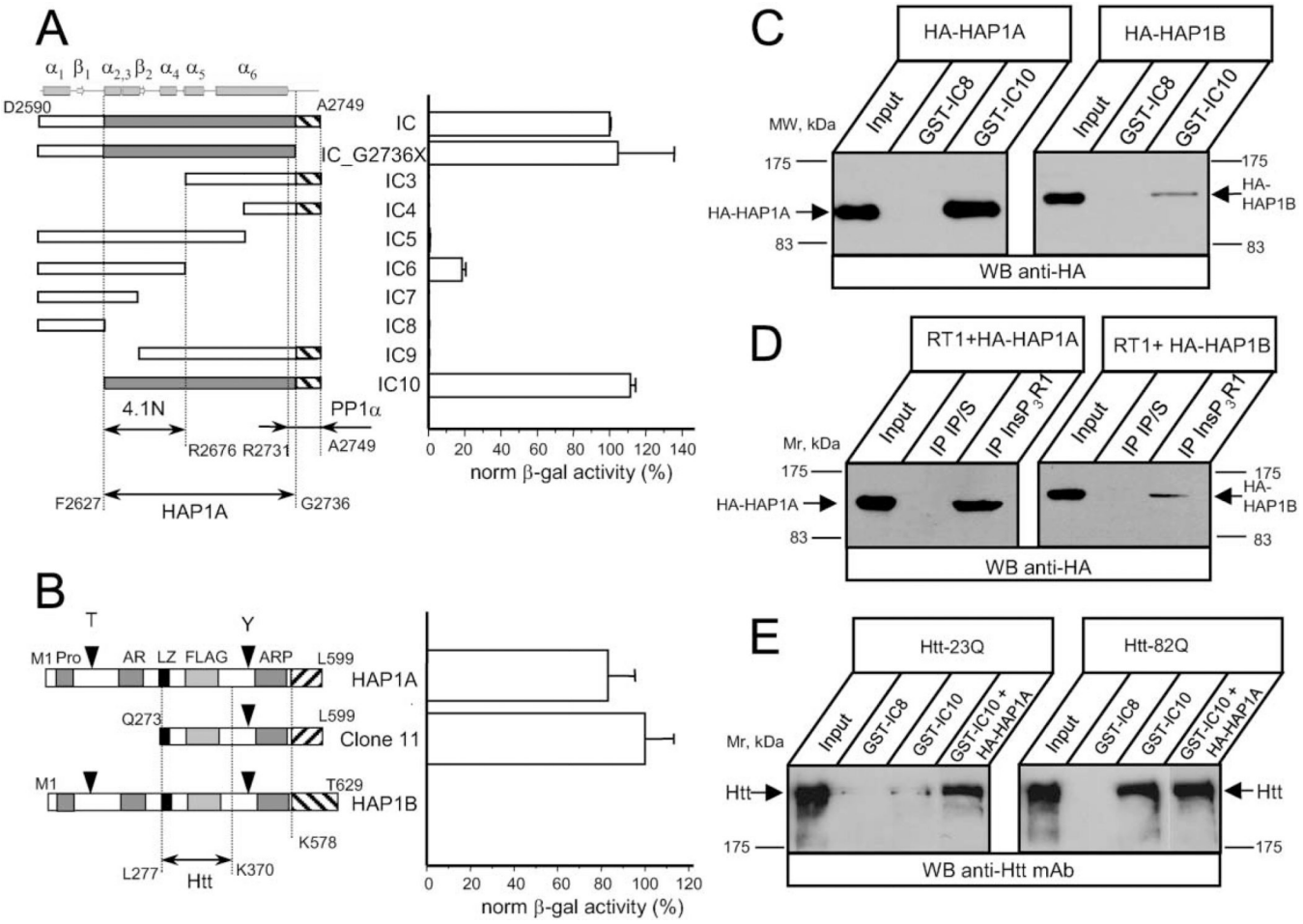

Figure 1. The $InsP_3R1$ Binds HAP1A and Htt in the Yeast Two-Hybrid System and In Vitro

(A) The strength of interaction between each $InsP_3R1$ IC bait and clone 11 (Q273–L599 of rat HAP1A) was determined by a liquid Y2H assay. The β-galactosiadase activity is plotted as a percentage relative to the IC/clone 11 interaction (mean ± SE, n = 3). On the top, predicted secondary structure elements within the IC sequence are shown. The predicted minimal fragment of the rat $InsP_3R1$ carboxy terminus (F2627–G2736) required for association with HAP1A is shaded. The minimal 4.1N binding domain (F2627–R2676) (Maximov et al., 2003) and minimal PP1α binding region (R2731–A2749) (Tang et al., 2003) are also shown.

(B) The strength of interaction between full-length rat HAP1A, rat HAP1B, and clone 11 with IC10 $InsP_3R1$ bait was determined by liquid Y2H assay. Data are presented in percentages relative to the observed interaction between clone 11 and IC10 (mean ± SE, n = 3). The carboxy-terminal regions unique to HAP1A and HAP1B isoforms are depicted by striped boxes. Also shown are the Htt binding region of HAP1 (L277–K370) (Li et al., 1995, 1998b) and motifs identified in HAP1 by computer analysis.

(C) GST-IC8/IC10 pull-down experiments of HA-HAP1A or HA-HAP1B from COS7 cells extracts.

(D) Lysates from RT1-infected Sf9 cells and COS7 cells overexpressing either HA-HAP1A or HA-HAP1B were mixed for 2 hr and analyzed by immunoprecipitation with anti-$InsP_3R1$ polyclonal antibodies or corresponding preimmune sera (IP/S).

(E) GST-IC8/IC10 pull-down experiments of Htt-23Q or Htt-82Q from HEK293 cells extracts. COS7 lysate containing overexpressed HA-HAP1A was added to GST-IC10 pull-

down reactions as indicated. The input lanes on (C)–(E) contain 1/50 of the COS7 and HEK293 cell lysates used in GST pull-down or immunoprecipitation experiments. The precipitated fractions were analyzed by Western blotting with anti-HA monoclonal antibodies (C and D), or anti-Htt monoclonal antibodies (E).

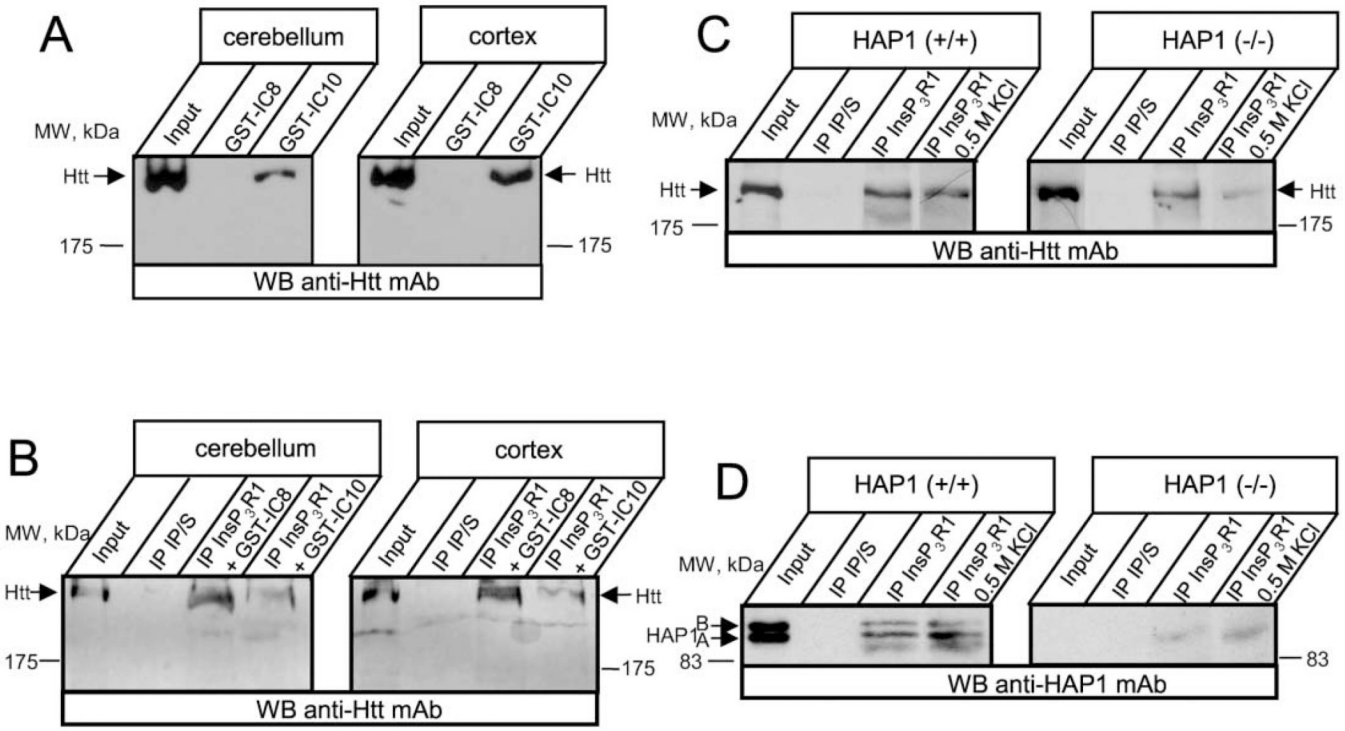

Figure 2. InsP$_3$R1 Is Associated with Htt In Vivo

(A) Rat cerebellar (left) or cortical (right) lysates were used in GST-IC8/IC10 pull-down experiments.

(B) Rat cerebellar (left) or cortical (right) lysates were used in coimmunoprecipitation experiments with anti-InsP$_3$R1 polyclonal antibodies or corresponding preimmune sera (IP/S). GST-IC8 and GST-IC10 proteins (200 μg/ml final concentration) were included in the immunoprecipitation reactions as indicated. The precipitated fractions on (A) and (B) were analyzed by Western blotting with anti-Htt monoclonal antibodies.

(C and D) Cortical lysates from wild-type (left panel) or HAP1$^{-/-}$ (right panel) mice (at postnatal day 3) were used in immunoprecipitation experiments with the anti-InsP$_3$R1 polyclonal antibodies or with the corresponding preimmune sera (IP/S). The precipitated proteins were analyzed by Western blotting with the anti-Htt monoclonal antibodies (C) or with the anti-HAP1 monoclonal antibodies (D). An additional 0.5 M KCl wash step was included in the immunoprecipitation protocol as indicated. The input lanes on (A)–(D) contain 1/50 of lysates used in immunoprecipitation and GST pull-down experiments.

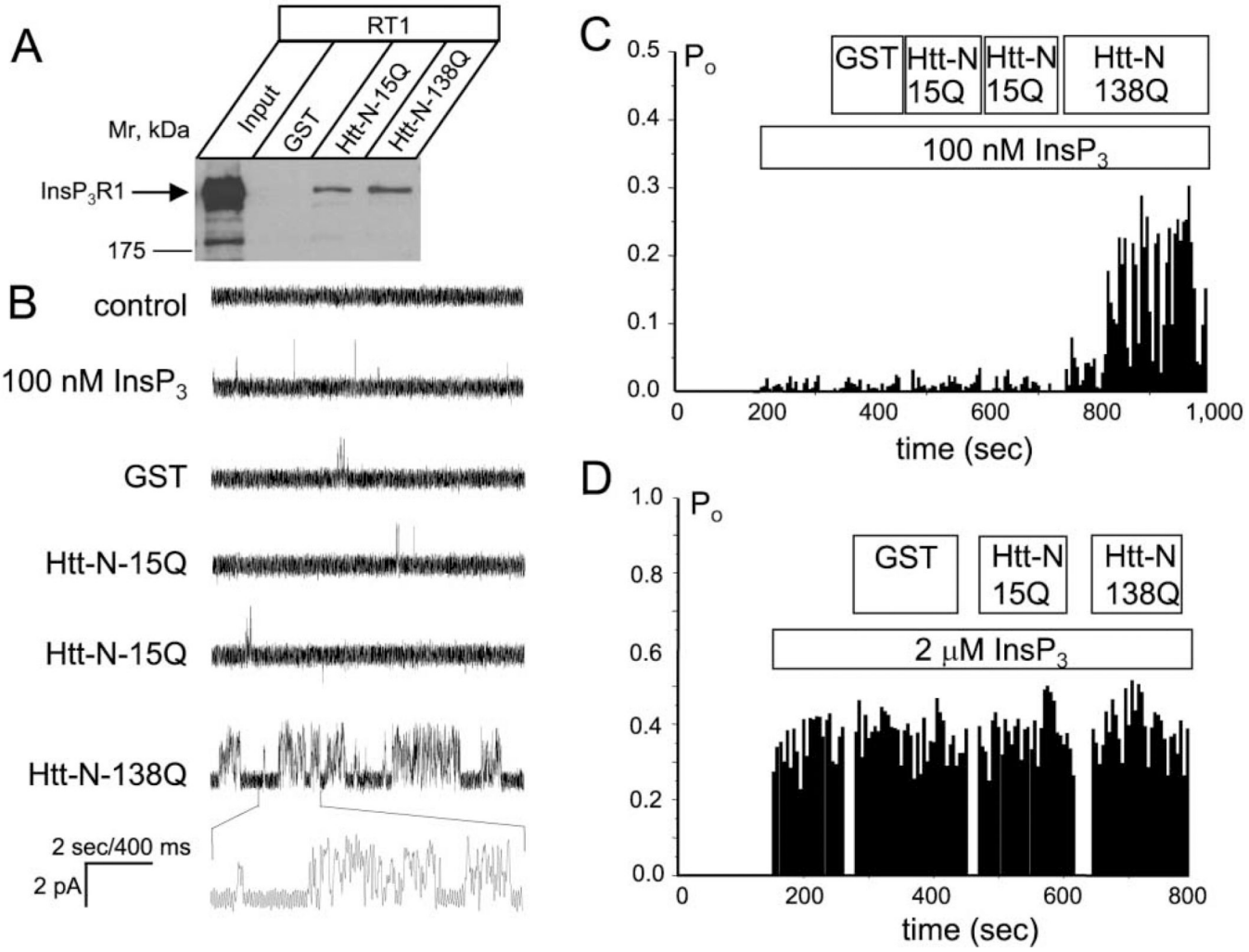

Figure 3. The Htt^{exp} Amino Terminus Sensitizes the InsP$_3$R1 to InsP$_3$

(A) Lysates from full-length InsP$_3$R1 (RT1)-infected Sf9 cells were used in pull-down experiments with GST, Htt-N-15Q, and Htt-N-138Q GST-fusion proteins as indicated. The precipitated fractions were analyzed by Western blotting with anti-InsP$_3$R1 polyclonal antibodies

(B) Effects of GST, Htt-N-15Q, and Htt-N-138Q on activity of recombinant InsP$_3$R1 in planar lipid bilayers at 100 nM InsP$_3$. Each current trace corresponds to 10 s (2 s for expanded traces) of current recording from the same experiment.

(C) The average InsP$_3$R1 open probability (P$_o$) in the presence of 100 nM InsP$_3$ is calculated for a 5 s window of time and plotted for the duration of an experiment. Data from the same experiment are shown on (B) and (C). Similar results were obtained in four independent experiments.

(D) The average InsP$_3$R1 P$_o$ plot for the experiment performed in the presence of 2 μM InsP$_3$. Similar results were obtained in two independent experiments. The times of InsP$_3$, GST, Htt-N-15Q, and Htt-N-138Q additions on (C) and (D) are shown above the P$_o$ plot.

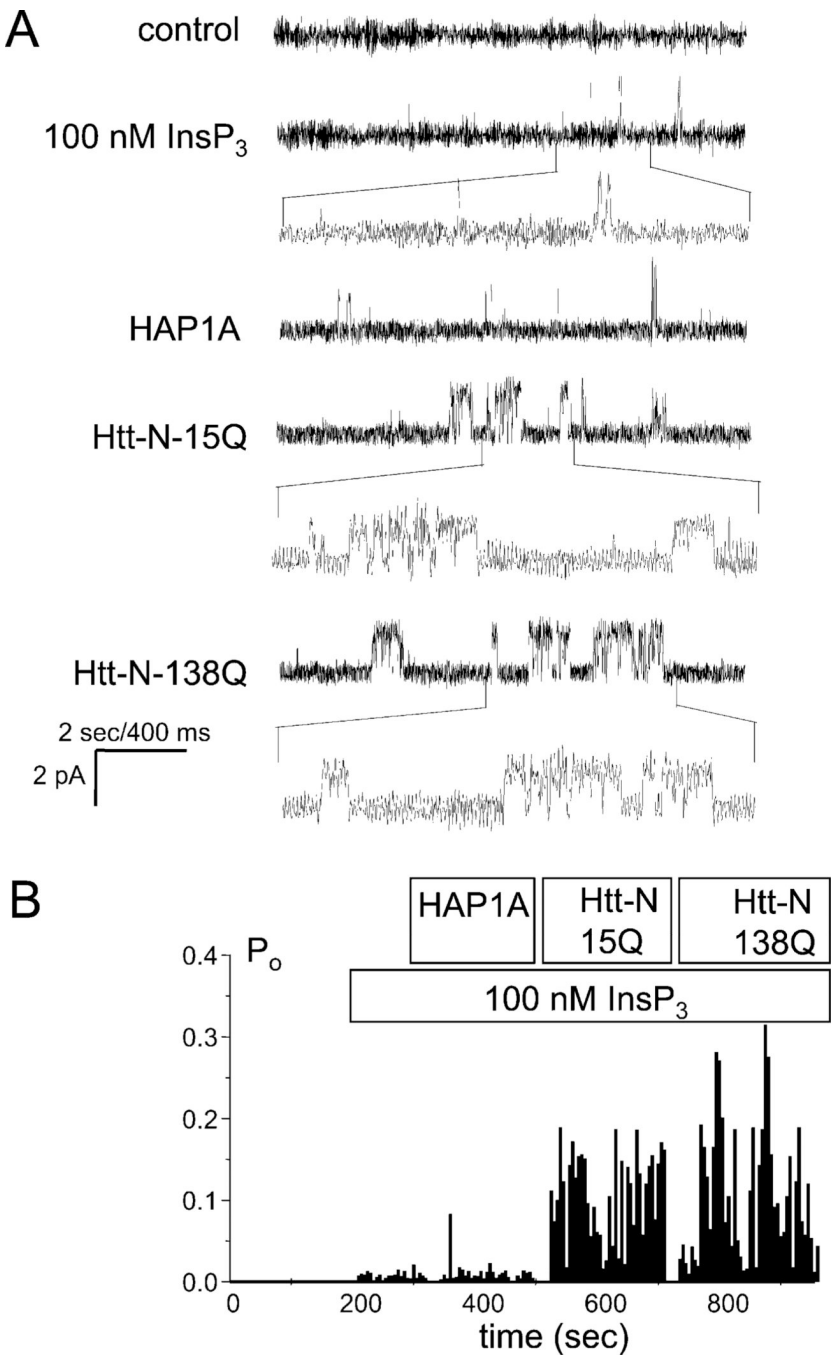

Figure 4. The Htt Amino Terminus Facilitates $InsP_3R1$ Activity in the Presence of HAP1A

(A) Effects of HAP1A, Htt-N-15Q, and Htt-N-138Q on activity of recombinant $InsP_3R1$ in planar lipid bilayers in the presence of 100 nM $InsP_3$. Each current trace corresponds to 10 s (2 s for expanded traces) of current recording from the same experiment.

(B) The average $InsP_3R1$ open probability (P_o) in the presence of 100 nM $InsP_3$ is calculated for a 5 s window of time and plotted for the duration of an experiment. The times of $InsP_3$, HAP1A, Htt-N-15Q, and Htt-N-138Q additions to the bilayer are shown above the P_o plot. Data from the same experiment are shown on (A) and (B). Similar results were obtained in two independent experiments or in experiments when HAP1A and Htt-N-15Q (n = 4) or HAP1A and Htt-N-138Q (n = 4) were premixed.

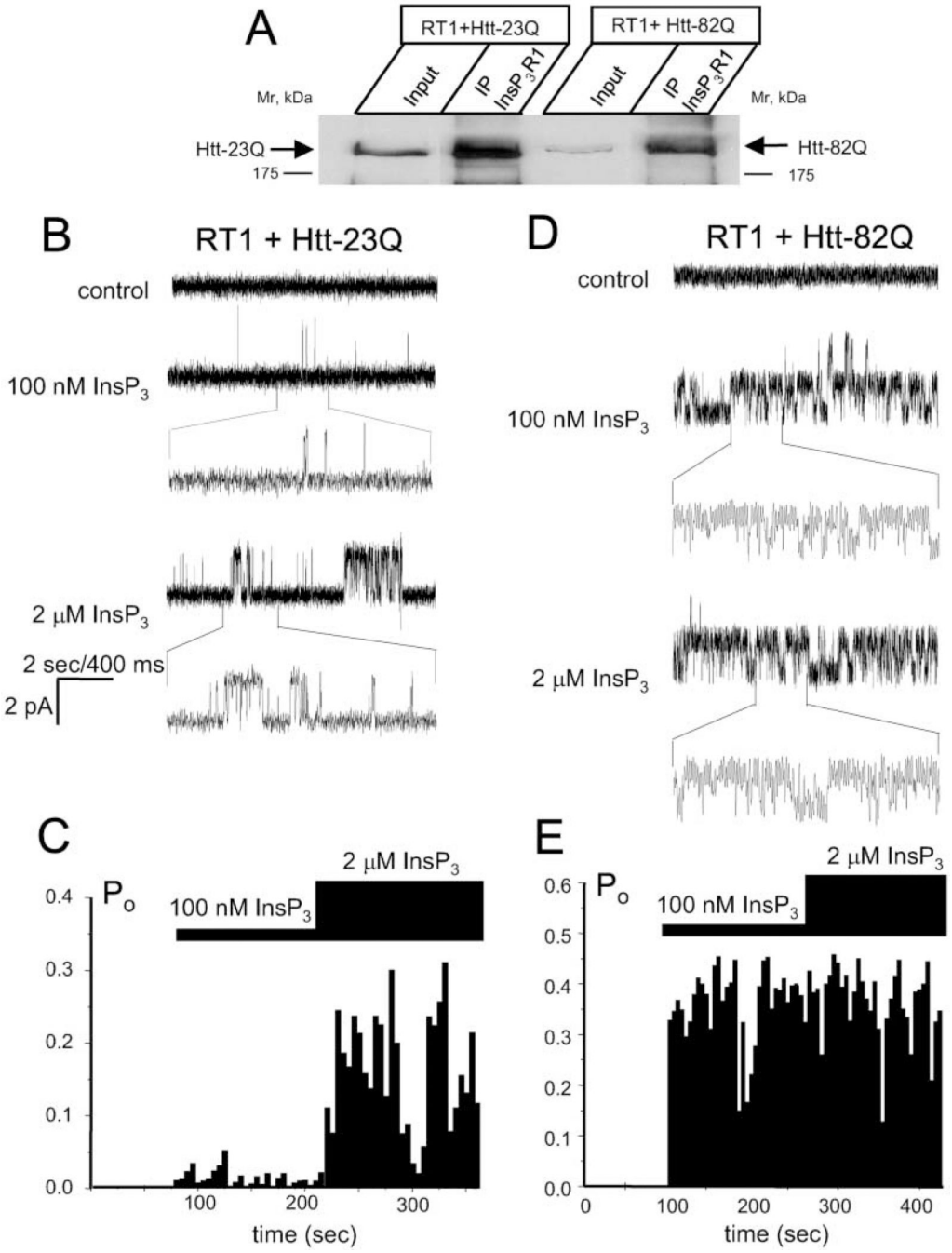

Figure 5. Full-Length Htt^{exp} Sensitizes InsP$_3$R1 to Activation by InsP$_3$

(A) Microsomes from Sf9 cells coinfected with RT1 and Htt-23Q or Htt-82Q baculoviruses were solubilzed in 1% CHAPS, precipitated with anti-InsP$_3$R1 polyclonal antibodies, and blotted with the anti-Htt monoclonal antibodies. The input lanes contain 1/10 of lysates used in the immunoprecipitation experiments.

(B) Activity of InsP$_3$R1 coexpressed in Sf9 cells with Htt-23Q and reconstituted into planar lipid bilayers. Responses to application of 100 nM InsP$_3$ and 2 μM InsP$_3$ are shown. Each current trace corresponds to 10 s (2 s for expanded traces) of current recording from the same experiment.

(C) The average $InsP_3R1$ open probability (P_o) was calculated for a 5 s window of time and plotted for the duration of an experiment. The times of 100 nM and 2 μM $InsP_3$ additions to the bilayer are shown above the P_o plot. Data from the same experiment are shown on (B) and (C). Similar results were obtained in four independent experiments.
(D and E) Same as (B) and (C) for $InsP_3R1$ coexpressed in Sf9 cells with Htt-82Q. Similar results were obtained in six independent experiments.

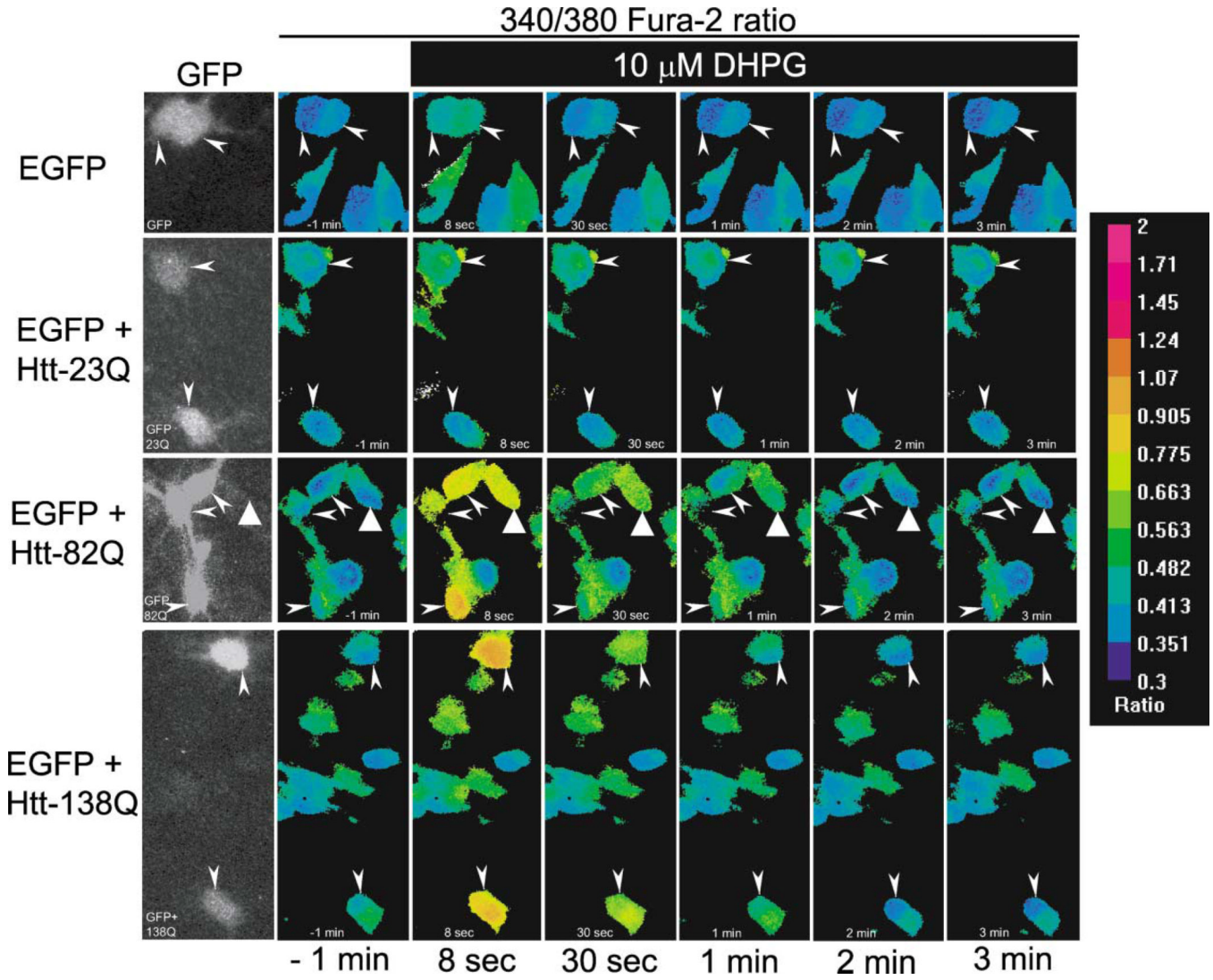

Figure 6. Effects of Htt^{exp} on DHPG-Induced Ca^{2+} Release in Transfected Medium Spiny Neurons

Representative images showing Fura-2 340/380 ratios in transfected rat medium spiny neurons (MSNs). The pseudocolor calibration scale for 340/380 ratios is shown on the right. Ratio recordings are shown for 10 μM DHPG-induced Ca^{2+} transients in MSN neurons transfected with EGFP (first row), EGFP + Htt-23Q (second row), EGFP + Htt-82Q (third row), and EGFP + Htt-138Q (fourth row). The recordings were performed in Ca^{2+}-free ACSF containing 100 μM EGTA. GFP images (1st column) were captured before Ca^{2+} imaging to identify transfected cells (arrowheads). 340/380 ratio images are shown for MSN neurons 1 min before (2nd column), and 8 s, 30 s, 1 min, 2 min, and 3 min after application of 10 μM DHPG as indicated. The GFP-negative cell that responds to 10 μM DHPG in the third row (triangle arrow) is interpreted to correspond to a neuron transfected with Htt-82Q plasmid alone. We used Htt:EGFP plasmids at a 3:1 ratio during transfections, which probably resulted in the expression of Htt in some GFP-negative MSNs. Only GFP-positive MSNs were considered for quantitative analyses shown on Fig 7.

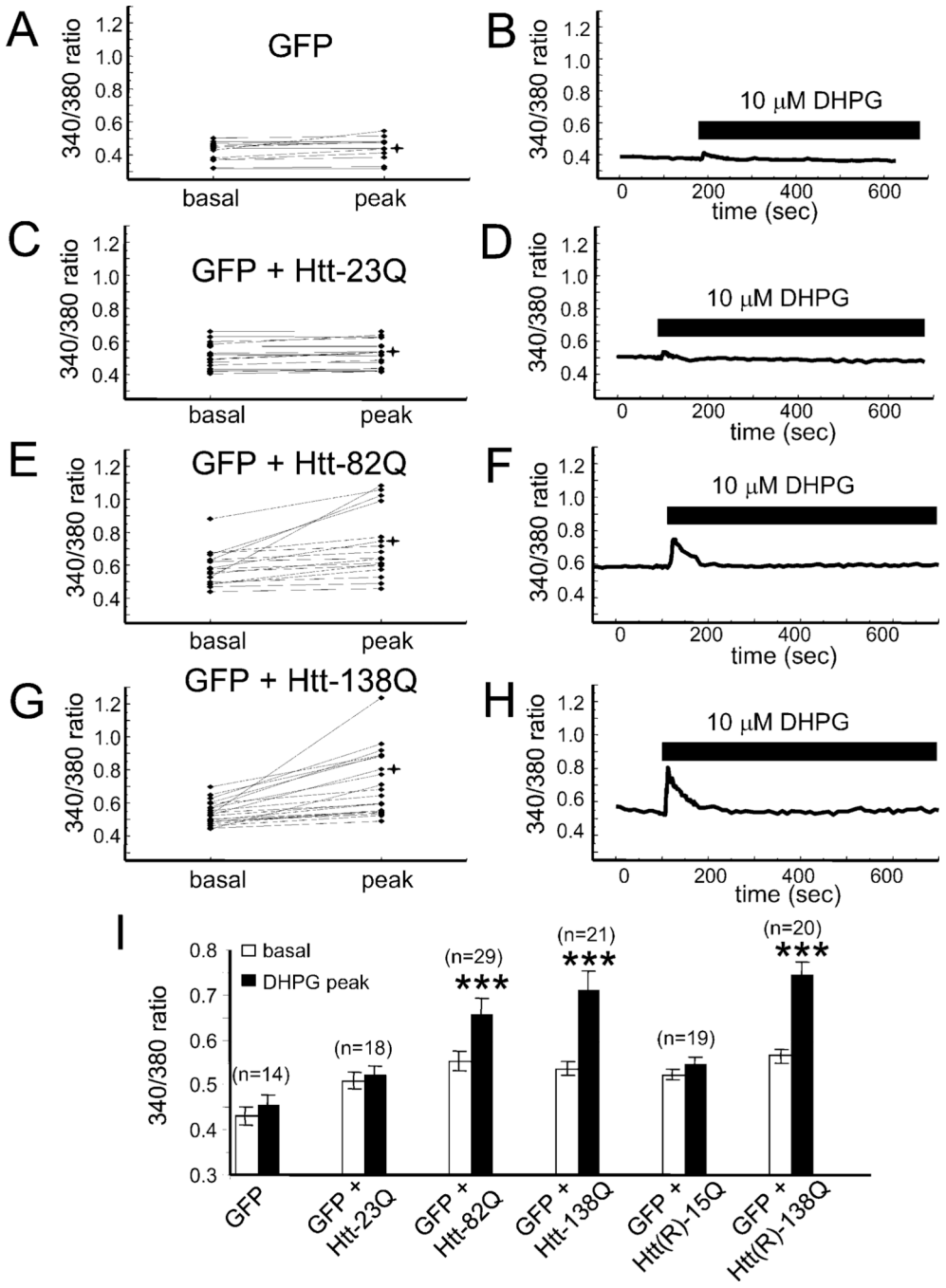

Figure 7. Htt^{exp} Facilitates DHPG-Induced Ca^{2+} Release in Medium Spiny Neurons

Basal and peak 340/380 ratios are shown for individual MSN neurons transfected with (A), EGFP, (C), EGFP+Htt-23Q, (E), EGFP+Htt-82Q, (G), EGFP+Htt-138Q. The experiments were performed as described in Figure 6. Only GFP-positive MSNs were considered for quantitative analysis for each group of cells. The basal ratios were determined 1 min prior to DHPG application (−1 min). The peak ratios were measured from maximal signals observed within 30 s after DHPG application. 340/380 ratio traces for representative cells (marked *) are shown in (B), (D), (F), and (H). Time of DHPG application is shown. Similar results were obtained in four independent transfections. (I) Summary of MSN Ca^{2+} imaging experiments with Htt and Htt(R) constructs. Average basal and DHPG-evoked peak 340/380

ratios from four independent transfections are shown as mean + SEM (n = number of cells). These averages represent the data shown in this figure in addition to data from other experiments. The peak ratios in MSNs transfected with EGFP + Htt-82Q, EGFP + Htt-138Q, or EGFP + Htt(R)-138Q are significantly (***$p < 0.001$, paired t test) higher than the basal ratios in the same cells.

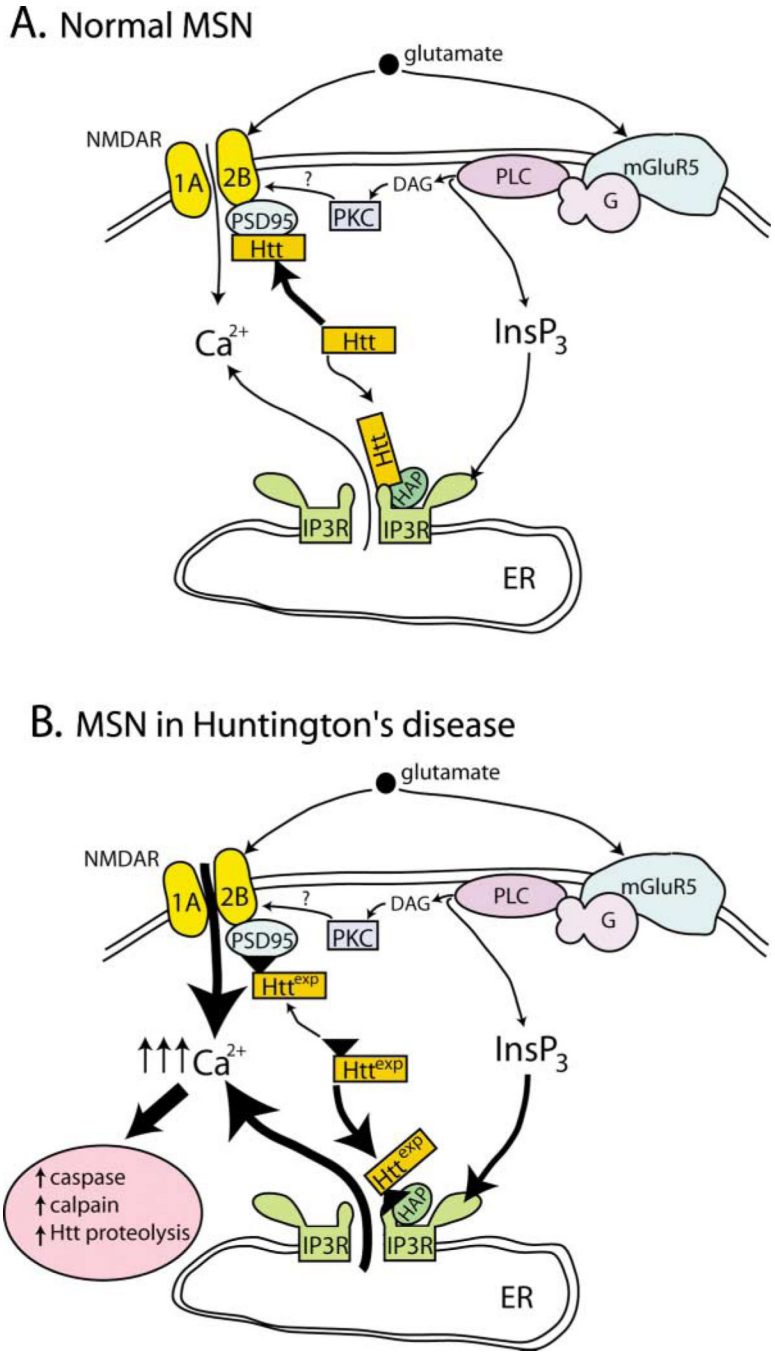

Figure 8. Proposed Mechanism Linking Htt^{exp} to Increased $InsP_3R1$- and NMDAR-Mediated Neuronal Ca^{2+} Signaling in Medium Spiny Neurons of HD Patients

Glutamate released from corticostriatal projection neurons stimulates NR1A/NR2B NMDAR and mGluR5 receptors on striatal medium spiny neurons (MSNs).

(A) In normal MSNs, NMDAR activation triggers Ca^{2+} influx from extracellular sources. Activation of mGluR5 stimulates phospholipase C (PLC) via a heterotrimeric G protein (G) pathway to generate diacylglycerol (DAG) and inositol triphosphate ($InsP_3$) second messengers. Activation of mGluR5 cooperates with NMDAR activation largely through the actions of DAG, which activates PKC. The $InsP_3$ generated downstream of mGluR5 does not trigger robust Ca^{2+} release from the endoplasmic reticulum (ER) in response to low

levels of glutamate, as $InsP_3R1$ sensitivity to $InsP_3$ is low. The association of Htt with the cytosolic carboxy-terminal tail of the $InsP_3R1$ is weak and with the PSD95-NR1A/NR2B is strong. In this schematic, only the interaction of Htt with the $InsP_3R1$ carboxy-terminal tail is represented. This interaction appears to be stabilized by the presence of HAP1A (labeled as HAP1) in normal MSNs.

(B) In MSNs of Huntington's disease (HD) patients, Htt^{exp} perturbs Ca^{2+} signaling via two synergistic mechanisms. Htt^{exp} enhances NMDAR function, possibly through decreased interaction with the PSD95-NR1A/NR2B complex. In addition, Htt^{exp} strongly binds to $InsP_3R1$ carboxy terminus and sensitizes the $InsP_3R1$ to activation by $InsP_3$. As a result, low levels of glutamate released from corticostriatal projection neurons lead to supranormal Ca^{2+} influx via NMDAR and Ca^{2+} release via the $InsP_3R1$. The net result is elevated intracellular Ca^{2+} levels in MSNs that eventually trigger pathogenic Ca^{2+}-dependent downstream pathways such as increased caspase and calpain activity, increased Htt proteolysis, activation of the apoptotic program, and MSN degeneration.